Journal of Nuclear Medicine, published on March 31, 2021 as doi:10.2967/jnumed.120.258814

GRPr antagonist ^{68}Ga-SB3 PET/CT-imaging of primary prostate cancer in therapy-naive patients

Ingrid L. Bakker[1], Alida C. Fröberg[1], Martijn B. Busstra[2], J. Fred Verzijlbergen[1], Mark Konijnenberg[1], Geert J. L. H. van Leenders[3], Ivo G. Schoots[1], Erik de Blois[1], Wytske M. van Weerden[2], Simone U. Dalm[1], Theodosia Maina[4], Berthold A. Nock[4], Marion de Jong[1]

1 Dept. of Radiology & Nuclear Medicine, Erasmus MC, Rotterdam, The Netherlands

2 Dept. of Urology, Erasmus MC, Rotterdam, The Netherlands

3 Dept. of Pathology, Erasmus MC, Rotterdam, The Netherlands

4 Molecular Radiopharmacy, INRASTES, NCSR "Demokritos", Athens, Greece

Corresponding author:

Marion de Jong

Erasmus MC, Room No Na2503

PO box 2040

3000 CA Rotterdam

The Netherlands

m.hendriks-dejong@erasmusmc.nl

First author:

Ingrid L Bakker, PhD student

Erasmus MC, Room No Na2503

PO box 2040

3000 CA Rotterdam

The Netherlands

i.l.bakker@erasmusmc.nl

Word count: 4958.

Running Title: Prostate cancer imaging using ^{68}Ga-SB3

ABSTRACT

The gastrin releasing peptide receptor (GRPr) is overexpressed in prostate cancer (PCa) cells, making it an excellent tool for targeted imaging. The gallium-68 labeled GRPr antagonist SB3 (^{68}Ga-SB3) has shown excellent results in (pre)clinical studies and was selected for further clinical investigation. The aims of this phase I study were to investigate ^{68}Ga-SB3 PET/CT-imaging of primary PCa tumors and assess safety. More aims included biodistribution, dosimetry, comparison with pathology and GRPr expression.

MATERIALS AND METHODS: Ten therapy-naive, biopsy-confirmed PCa patients planned for prostatectomy were included. A 3-hour extensive PET/CT-imaging protocol was performed, within 2 weeks prior to prostatectomy. Prostate tissue was evaluated for tumor localization, Gleason Score and in vitro autoradiography was performed to determine GRPr expression. Available MRI scans performed within 3 months prior to the study were matched. For dosimetry residence times were estimated and effective dose to the body as well as absorbed doses to organs were calculated using the IDAC dose 2.1 model.

RESULTS: Administration of ^{68}Ga-SB3 (187.4 ± 40.0 MBq, 40±5 μg) was well tolerated, no significant changes in vital signs or laboratory results were observed. ^{68}Ga-SB3 PET/CT showed lesions in 8 out of 10 patients. Pathological analysis revealed a total of 16 tumor lesions of which PET/CT showed 14, resulting in a sensitivity of 88%. ^{68}Ga-SB3 PET/CT-imaging showed uptake in 2 large prostatic intraepithelial neoplasia foci, considered a precursor of PCa, resulting in an 88% specificity. Autoradiography of tumor lesions revealed heterogeneous GRPr expression and was negative in 4 patients. Both PET/CT-negative patients had a GRPr-negative tumor. In autoradiography-positive tumors, level of GRPr expression showed significant correlation to tracer uptake on PET/CT. Dosimetry calculations estimated the effective dose to be 0.0144 mSv/MBq, similar to other ^{68}Ga labeled radiopeptides. Highest absorbed dose was detected in the physiological GRPr-expressing pancreas (0.198 mGy/MBq), followed by bladder wall and kidneys.

CONCLUSION: ^{68}Ga-SB3 PET/CT is a safe imaging method and a promising tool for early PCa imaging.

KEYWORDS: Gastrin releasing peptide receptor, prostate cancer, tumor-imaging, positron emission tomography/computed tomography

INTRODUCTION

The gastrin-releasing peptide receptor (GRPr) is a promising tumor target, showing overexpression in multiple cancer types, among which prostate cancer (PCa), breast cancer and colon cancer (*1*).

Physiological GRPr expression is found throughout the gastro-intestinal (GI) tract and pancreas (*2*). Well-differentiated PCa shows higher receptor density than poorly differentiated tumors and an inverse correlation was found for GRPr expression, Gleason score (GS) and tumor size (*3*). Also, GRPr expression is present in high grade prostatic intraepithelial neoplasia (PIN), which is considered a precursor for PCa, with GRPr levels approaching those in PCa (*3*). Therefore, GRPr targeting tracers can offer new opportunities for staging and therapy monitoring of PCa.

Multiple GRPr binding agonists and antagonists have been synthesized for both imaging and therapy purposes (*4*). We selected the GRPr antagonist SB3 (DOTA-*p*-aminomethylaniline-diglycolic acid-DPhe-Gln-Trp-Ala-Val-Gly-His-Leu-NHEt) for further clinical investigation after promising preclinical and initial clinical results (*5,6*). SB3 is chemically based on the previously evaluated ^{99m}Tc-Demobesin1 (^{99m}Tc-N_4´-DPhe6-Gln-Trp-Ala-Val-Gly-His-Leu-NHEt; N4´= 6-{p-[(carboxymethoxy)acetyl]-amino-benzyl}-1,4,8,11-tetraazaundecane) showing high tumor uptake and retention and fast background clearance(*7*). The ^{99m}Tc-binding N_4´ chelator was replaced by a DOTA-chelator, enabling theranostic applications.

The primary aims of this phase I clinical study were to investigate the feasibility of imaging primary PCa using ^{68}Ga-SB3 PET/CT and to assess its safety. We tested ^{68}Ga-SB3 imaging by comparing pre-operative PET/CT-imaging with histopathological data of the prostatectomy tissue. Other objectives included determining biodistribution, pharmacokinetics, dosimetry, GRPr expression in tissue samples, and comparison with the standard of care multiparametric MRI.

MATERIALS & METHODS

Patients

The study was approved by national and local ethics committees and registered under EudraCT no 2011-005859-13. All patients gave written informed consent. Ten newly diagnosed therapy-naive biopsy-proven PCa patients scheduled for curative prostatectomy, were included in the study. If lower limit of detection was reached, defined by inability to evaluate visualization of physiological uptake, the patient was excluded from the study and replaced.

Tracer synthesis and radiolabeling

As SB3 (*8*) is a non-industry-sponsored compound, the Investigational Medical Product Dossier, Investigational Brochure and the production were approved under local and national supervision. GMP-grade SB3 was produced by piCHEM GmbH (Raaba-Grambach, Austria) and SB3 single-dose kits containing 50 µg SB3 in 100 µL 0.01 N acetic acid were produced by the GMP-licensed Erasmus MC Hospital Pharmacy.

Labeling of SB3 with ^{68}Ga was performed using Scintomics robotics (Fürstenfeldbruck, Germany), labeling solutions were provided by ABX (Radeberg, Germany). The eluate from a ^{68}Ge/^{68}Ga (Eckert & Ziegler, Berlin, Germany) generator was purified, concentrated and added to a reaction vial together with the SB3 kit dissolved in 3.0 mL 1.5 M HEPES. The mixture was heated for 10 min at 90°C and allow to cool for 5 min, purified on a Sep-Pak C_{18} cartridge (Waters, Etten-Leur, The Netherlands) and passed through a sterile 0.2 µm Cathivex GV filter (Merck KGaA, Darmstadt, Germany).

Safety

Vital functions were registered, blood sample were collected before, during and after administration of the radiopharmaceutical. Adverse effects were followed up until surgery.

^{68}Ga-SB3 PET/CT-imaging and biodistribution

The imaging study was performed on PET/CT (Biograph mCT, Siemens, Erlangen, Germany) within two weeks prior to surgery. An extensive scan protocol was performed see *Figure 1A* and *Supplemental table 1*. All PET acquisitions were preceded by a low dose CT scan.

PET images were reconstructed using an ordered subset expectation maximization algorithm using resolution recovery and time-of-flight information. Quantification of uptake was expressed by standardized uptake values (SUV).

To enable optimal imaging of the prostatic region, 40 mg furosemide was administered at 25 min.p.i., continuous flushing of the bladder was performed.

PET/CT-images were independently evaluated by two experienced nuclear medicine physicians (AF, JV) on an OsiriX 5.9 (Pixmeo Sàrl, Bernex, Switzerland) workstation and consensus was reported. PET-positivity was defined as focal tracer uptake in the prostate region, consistent over time and scored as 4 or 5 according to a 5-point Likert Score.

Volumes-of-interest (VOI) were drawn on ^{68}Ga-SB3 PET/CT fusion images in different volumes depending on the organ of interest. VOIs were positioned by an experienced clinical researcher (IB) and checked by a nuclear medicine physician (AF). Average SUV (SUV_{MEAN}) and maximum SUV (SUV_{MAX}) in VOIs were measured. Statistical differences in SUV between VOIs were calculated using two-tailed paired t-test.

Histopathological analysis

All patients underwent robot-assisted radical prostatectomy, some included extended pelvic lymph node dissection. Tissue was processed according to standard of care, shown in *Figure 1B* and *Supplemental figure 1*. Delineation of tumor foci, PIN and benign prostate hyperplasia was manually performed by an experienced pathologist (GvL). ^{68}Ga-SB3 PET/CT-imaging was correlated with pathological findings by a nuclear medicine physician and pathologist (AF, GvL) in consensus.

Autoradiography

The GRPr antagonist JMV4168 (DOTA-βAla-βAla-[H-d-Phe-Gln-Trp-Ala-Val-Gly-His-Sta-Leu-NH_2]) was labeled with Indium-111 as previously described (*9*). Fresh frozen prostate tissue sections of 10 µm were incubated 1.0 h with 300 µL 10^{-9} M ^{111}In-JVM416, and blocking studies were performed using either a 1000 fold excess of Tyr^4-BBN or SB3. Subsequently, phosphor screens were superimposed for 7 days, read on a Cyclone (Perkin Elmer) and tracer binding was quantified as digital lights units per mm^2 (DLU/mm^2) using OptiQuant software (Perkin Elmer, Waltham, United states).

Delineation of tumor was done by a pathologist (GvL) on adjacent stained tissue slides. Percentage of specific GRPr-positive areas within marked tumor was scored and evaluated by two independent readers (IB, SD), consensus was reported. The level of ^{111}In-JVM4168 binding of tumor areas was quantified and correlated, using Pearson's correlation coefficient, with the SUV_{MAX} of corresponding tumor lesion on ^{68}Ga-SB3 PET/CT-imaging.

Metabolic stability and pharmacokinetics

Blood samples and urine samples were collected at multiple timepoints (*Supplemental table 2*). Radioactivity and degradation of the compound was measured in a gamma-counter (1480 WIZARD automatic γ-counter, PerkinElmer, Waltham, United states). Registration of metabolites was performed as previously described (*6*).

Dosimetry

For organs of interest time-activity curves (TAC) were fitted using SUV_{MEAN} values to estimate organ residence times (Prism, GraphPad Software, La Jolla California USA). Goodness of fit was expressed by the R^2 metric, minimum R^2 of 0.8 was accepted. Bladder TAC was calculated using the Medical Internal Radiation Dose (MIRD) dynamic bladder model (*10*) with a one-hour voiding interval. Bone marrow TAC was calculated as previously described (*11*). Total activity per source organ, absorbed doses and effective dose were calculated according to ICRP 103 and 133.

Magnetic resonance imaging

The reports of recent MRI scans performed in clinical staging (within 3 months prior to study) were selected from the patient files, therefore blinded from PET/CT and histopathology results of biopsies and radical prostatectomy. The multiparametric MRI protocol was performed as standard of care after administration of a gadolinium-based contrast agent on a 3.0 T MRI (Discovery MR750, General Electric Healthcare, USA) using a 32-channel pelvic phased-array coil. MRIs were reviewed by an experienced urogenital radiologist (IS). Individual lesions were scored according to the Prostate Imaging Reporting and Data System (PI-RADS) version 2 guidelines.

RESULTS

Patients

Lower limit of detection was reached at 1.3 MBq/kg, this patient was excluded and replaced, a total of ten patients were included. Five patients also underwent an extended pelvic lymph node dissection.

Average age was 64.1 ± 7.8 years. PSA levels were 14.3 ± 7.9 µg/L (range 4 to 24.8) with clinical stages 4x T1c, 4x T2a, 1x T2c and 1x T3a. Evaluation of the biopsy cores showed 2x GS 3+3=6, 6x GS 3+4=7, 1x GS 4+3=7 and 1x GS 4+4=8. See *Supplemental table 3*.

Tracer synthesis and radiolabeling

All radiolabeling procedures yielded a radiochemical purity of >90%, radiochemical incorporation of >99%, the product was sterile and free of bacterial endotoxins.

Safety

Administration proceeded without adverse events. Eight patients experienced discomfort of the flush catheter, including bladder cramps. Catheter position and flush volume were adjusted to relieve symptoms. In one patient one scan was omitted to allow for adjustments, not reducing evaluability of the patient.

Full gastrin panels were determined in 8 patients, they showed peak levels 30 min.p.i. and a steady decline corresponding to normal 60 minutes postprandial gastrin levels. The peak levels were 100 ± 50 ng/L, comparable to earlier findings of 157.8 ± 67.5 ng/L in healthy persons (*12*).

^{68}Ga-SB3 PET/CT-imaging and biodistribution

Patients received 187 ± 40 MBq (range 130-260 MBq), 40 ±5 µg ^{68}Ga-SB3; 2.2 ± 0.5 MBq/kg. ^{68}Ga-SB3 PET/CT visualized lesions in 8 of 10 patients, two examples are shown in *Figure 2 and 3*. Total body PET images of all patients can be found in *Supplemental figure 2*. A total of 24 potential tumor lesions were identified in the prostate (*Table 1*). Two patients were suspected of lymph node metastases.

One unanticipated incidental finding was a sphere-like lesion within the cranium, SUV at level of blood, suspected of a hemangioma, see *Supplemental figure 3*. MRI confirmed the diagnosis.

A total of 1522 VOIs were drawn in 93 scans, see *Figure 4* and *Supplemental table 4*. The average SUV_{MAX} of suspected tumor lesions was 7.1 ± 4.8 at 60 min.p.i. (median 5.5, range 3.2 – 22.7). Average tracer uptake in tumor lesions on all timepoints was 3.3 times higher compared to that in normal prostate tissue (95% CI: 2.9 – 3.7). SUV_{MEAN} showed the same overall distribution as SUV_{MAX}.

High radioactivity was found in kidneys (SUV_{MAX} 4.1 ± 0.9 at 60 min.p.i.) and urinary tract. Intense physiological uptake was observed in the GRPr-expressing pancreas (SUV_{MAX} 42.1 ± 15.7 at 60 min.p.i.). Interestingly, a significantly higher uptake was found in the head of the pancreas compared to the tail at all timepoints, with an average difference of 9.1 SUV_{MAX} $p < 0.001$ (head SUV_{MAX} 46.3 ± 13.8; tail SUV_{MAX} 36.4 ± 16.9 at 60 min). Diffuse uptake was seen throughout the GI-tract, more pronounced uptake in lower esophageal sphincter and anal sphincter complex. Little physiological uptake was seen in thyroid, liver and spleen (SUV_{MAX} < 2 at 60 min.p.i.) similar to background tissue.

Histopathological analysis and correlation to ^{68}Ga-SB3 PET/CT-imaging

A total of 16 tumor lesions were found in the prostatectomy specimens. In six patients two separate tumor lesions were identified, with different GS in two patients (*Table 1*).

Correlation of histopathological data with ^{68}Ga-SB3 PET/CT-imaging revealed two false-negative tumors; one was a very small, diffuse-growing GS 3+3=6 tumor, the other was a large solid GS 3+4=7 tumor. Most PIN lesions were found adjacent to tumor foci and were not separately evaluated. Interestingly, two focal hotspots on ^{68}Ga-SB3 PET/CT-images were identified as two relatively large solitary PIN fields of >5 mm diameter (*Figure 5*). The sensitivity of ^{68}Ga-SB3 PET/CT for detection of PCa on a lesion basis was 88% (14/16), specificity 88% (14/16).

Pathology and ^{68}Ga-SB3 PET/CT revealed lymph node metastases in the same two patients, however lesion-based validation was not achievable.

Autoradiography

Autoradiography with ^{111}In-JVM4168 showed GRPr binding in tumor foci of all patients, although sometimes only very small tumor foci were observed. Blocking studies confirmed specific uptake *Supplemental figure 4*. The GRPr expression of tumor was homogenous in two patients,

heterogeneous in four patients and autoradiography was negative in four patients. Of this last group, 2 patients also had negative ^{68}Ga-SB3 PET/CT.

Quantification of GRPr binding in tumor areas was determined and compared to the SUV_{MAX} of likely corresponding tumor lesion om ^{68}Ga-SB3 PET/CT imaging, showing a significant correlation Pearson $r^2 = 0.88$ $p < 0.05$ (*Supplemental figure 5*).

Metabolic stability and pharmacokinetics

The radiopeptide proved to be very stable in blood (86.4 ± 11.0% at 10 min.p.i.). It showed little to no degradation in urine (92.1 ± 7.1 % at 60 min.p.i.).

Renal clearance showed a bi-exponential excretion curve: a fast excretion phase (90%) with a biological half-life ($t_{½}$) of 6 min and the remainder with $t_{½}$ 242 min. Pancreas and prostate showed mono-phasic excretions with a $t_{½}$ 180 and 135 min, respectively. An uptake-and-excretion curve was fitted for the tumor with a $t_{½}$ 235 min for the excretion phase (*Figure 6*).

Dosimetry

Residence times and absorbed doses are described in *Supplemental table 5*. The pancreas showed the highest absorbed dose of 198 µGy/MBq, followed by ureters, bladder wall and kidneys (134, 116 and 53 µGy/MBq, respectively). Assuming a one-hour voiding model, we estimated an effective dose of 14.4 µSv/MBq, corresponding to 2.66 ± 0.56 mSv in our patients.

Magnetic Resonance Imaging

Eight patients had a diagnostic MRI report on file, which revealed 10 tumor foci: 3x PIRADS 3, 3x PIRADS 4 and 4x PIRADS 5. Lesions described on MRI were correlated to ^{68}Ga-SB3 PET/CT in 10 of 13 lesions in 8 of 8 patients (*Table 1*). Only one lesion identified by MRI, was not detected by PET/CT which corresponded with a GRPr-negative tumor on autoradiography. Three lesions that were found on PET/CT were not explicitly described by MRI; data was not adequate to determine if these were true false negatives.

DISCUSSION

Currently, multiple radiopharmaceuticals are available for imaging of PCa, predominantly PSMA-targeting compounds, the long-established choline, fluciclovine and GRPr-targeting compounds (*13*). PSMA tracers have been proposed to replace choline-based tracers in the current PCa guideline (*14*). However, limitations for PSMA tracers are still apparent with respect to the sensitivity of early stage, low GS tumors (*15*).

Several GRPr antagonists have been tested in the clinical setting, such as RM2, MJ9, DOTAGA-PEG-RM26 and NeoBOMB1, all coupled to the short living Gallium-68 (*4,16-18*). In a head-to-head comparison in a small patient group, GRPr tumor imaging was comparable to PSMA (*19*).

With regards to safety, a peptide dose up to 45 μg SB3 revealed no serious adverse effects. As expected, the pancreas and urinary tract received the highest absorbed dose, similar to previously reported Gallium-68 GRPr antagonists (*16,18*).

^{68}Ga-SB3 PET/CT visualized tumor foci in 8 out of 10 patients. One PET-negative patient had a very small, GS 3+3=6, diffuse-growing tumor. Considering the average range of Gallium-68-produced positrons (1.05 mm in soft tissue), a partial volume effect is expected in small tumors. However, in a clinical setting it is debatable whether detection of such small tumor foci is relevant. The other PET-negative patient had a large, GS 3+4=7, solid-growing tumor, which autoradiography conformed to be GRPr negative. GRPr expression in primary PCa is present in 90-100% (*3,20*).

When comparing ^{68}Ga-SB3 to another clinically tested GRPr antagonist, ^{68}Ga-RM2 performance was comparable: SUV_{MAX} 7.1 vs 9.1 at 60 min.p.i.; sensitivity 88% vs 85%, respectively (*21*). We found no clear correlation between SUV_{MAX} and GS scale (p=0.11) nor PSA levels (p=0.80), consistent with ^{68}Ga-RM2.

It was reported that in high grade PIN, considered a precursor for PCa, GRPr expression levels on autoradiography approached that of PCa (*3*). Although, these findings have been challenging to reproduce in a clinical setting. Classification of PIN is difficult, and it is mostly located amidst or adjacent tumors. We found two relatively large areas of PIN separate from the tumor in one patient, that were visualized as well as PCa by ^{68}Ga-SB3. We found no published data of similar compounds binding to PIN in a clinical setting to date.

The two patients suspected of lymph node metastases on ^{68}Ga-SB3 PET/CT were confirmed by pathology. However, the protocol was not designed to compare lymph node location in histopathology and PET/CT, and with only two patients these findings should be considered preliminary.

The diffuse low uptake throughout the GI-tract may be underestimated because of partial volume effect and bowel movement. The higher uptake in lower esophageal sphincter and anal sphincter complex has been described in GRPr imaging before (*5,22*), most likely due to presence of GRPr in smooth muscle cells (*23*). Uptake pattern was comparable to ^{68}Ga-RM2, with comparable pancreatic uptake around 50 SUV_{MAX} at 60 min.p.i. (*21*).

The administration of furosemide, resulted in faster renal clearance, but otherwise did not significantly alter tracer uptake in kidneys.

To our knowledge, this is the first study that showed a significant difference of GRPr uptake between the head and tail of the pancreas. Compared to the head, the corpus and tail have different embryological origins (*24*), which may explain difference in cell characteristics. However function of GRPr in the pancreas has not yet been described.

The high absorbed pancreatic dose might be a concern for therapy. Gnesin et al. predict an absorbed pancreatic dose of 1.85 Gy for a theoretical 7.4 GBq ^{177}Lu-labeled MJ9 administration. We published an estimated pancreatic dose of 0.20 mGy/MBq corresponding to 1.48 Gy for the same administration. This can be considered safe when comparing to external beam radiotherapy (*18,25*).

Low GS PCa follows the ductal pattern of regular prostate anatomy, which can present as dots in a trans-axial slide, and variation of GRPr expression levels per tumor can contribute to heterogeneous expression patterns. In two patients we found good ^{68}Ga-SB3 PET/CT-imaging while autoradiography showed GRPr-negativity, probably due to small sample size of frozen sections.

Currently MRI is used for local staging of PCa. ^{68}Ga-SB3 PET/CT performed equally well in local staging of tumor lesions in this small group. However, because of low spatial resolution PET-imaging will not be useful for determining local invasion.

Previous results with ^{68}Ga-SB3 PT/CT-imaging in progressive disseminated recurrent prostate cancer patients with history including anti-hormonal therapy, which could impact GRPr expression, showed a sensitivity of 55% (*5*). The excellent stability and tumor to background ratios we found,

combined with the relative slower washout of the tumor lesions is encouraging for the prospect of therapeutic application. ^{177}Lu-SB3 was evaluated in animal studies, where it showed poor in vivo stability. However, this effect could be fully prevented by co-injecting the endopeptidase inhibitor phosphoramidon (*26*). No clinical data is available yet.

The main limitations of this study are small number of patients and the varying patient population. Clearly, more clinical studies should be conducted to define the potential theranostic value of this compound.

Conclusion

The GRPr antagonist ^{68}Ga-SB3 has shown excellent imaging qualities and is safe to use in primary PCa patients with high sensitivity for early stage PCa. ^{68}Ga-SB3 has an attractive biodistribution pattern with fast renal clearance and relatively long tumor retention.

Disclosures

No potential conflict of interest to this study was reported.

Acknowledgements

The authors would like to thank all employees of the department of Radiology and Nuclear Medicine at Erasmus for their collaborative effort to realize this locally sponsored radiolabeled drug research. In particular W.A.P. Breeman P.J.J.M. Janssen and M. van der Meij aiding in IMPD and IB completion, J. Teunissen our independent physician, the scan team: F. van der Pluijm, G. Caan, T. Cox and A.S. Almeida. We thank H. Voorwinden and J. de Swart for radiation protection advice and the whole radiolabeling team for their efforts and the Radiology Trial Office for monitoring. Special thanks to E. Holleman for insights in interpreting pathology data.

At time of submission Fred Verzijlbergen is employed at Radboud University, Nijmegen, The Netherlands.

Key Points

QUESTION: Is the use of GRPr antagonist ^{68}Ga-SB3 safe and is PET/CT-imaging of primary prostate cancer sensitive and accurate?

PERTINENT FINDINGS: This clinical trial in a small patient group proceeded without adverse events and it showed a sensitivity of ^{68}Ga-SB3 PET/CT-imaging of 80% on patient basis. It has an attractive biodistribution pattern with fast renal clearance and relatively long tumor retention. The two PET/CT-negative patients were confirmed to have a GRPr-negative tumor.

IMPLICATIONS FOR PATIENT CARE: ^{68}Ga-SB3 PET/CT is a promising tool for early prostate cancer imaging, with further research it could aid in staging of primary disease.

REFERENCES

1. Cornelio DB, Roesler R, Schwartsmann G. Gastrin-releasing peptide receptor as a molecular target in experimental anticancer therapy. *Ann Oncol.* 2007;18:1457-1466.
2. Jensen RT, Battey JF, Spindel ER, Benya RV. International Union of Pharmacology. LXVIII. Mammalian bombesin receptors: nomenclature, distribution, pharmacology, signaling, and functions in normal and disease states. *Pharmacol Rev.* 2008;60:1-42.
3. Markwalder R, Reubi JC. Gastrin-releasing peptide receptors in the human prostate: relation to neoplastic transformation. *Cancer Res.* 1999;59:1152-1159.
4. Baratto L, Jadvar H, Iagaru A. Prostate cancer theranostics targeting gastrin-releasing peptide receptors. *Mol Imaging Biol.* 2018;20:501-509.
5. Maina T, Bergsma H, Kulkarni HR, et al. Preclinical and first clinical experience with the gastrin-releasing peptide receptor-antagonist ^{68}Ga-SB3 and PET/CT. *Eur J Nucl Med Mol Imaging.* 2016;43:964-973.
6. Bakker IL, van Tiel ST, Haeck J, et al. In vivo stabilized SB3, an attractive GRPR antagonist, for pre- and intra-operative imaging for prostate cancer. *Mol Imaging Biol.* 2018;20:973-983.
7. Nock B, Nikolopoulou A, Chiotellis E, et al. ^{99m}Tc-Demobesin 1, a novel potent bombesin analogue for GRP receptor-targeted tumour imaging. *Eur J Nucl Med Mol Imaging.* 2003;30:247-258.
8. Maina T, Nock BA. From bench to bed: New gastrin-releasing peptide receptor-directed radioligands and their use in prostate cancer. *PET Clin.* 2017;12:205-217.
9. Marsouvanidis PJ, Nock BA, Hajjaj B, et al. Gastrin releasing peptide receptor-directed radioligands based on a bombesin antagonist: synthesis, ^{111}In-labeling, and preclinical profile. *J Med Chem.* 2013;56:2374-2384.

10. Thomas SR, Stabin MG, Chen CT, Samaratunga RC. MIRD Pamphlet No. 14 revised: A dynamic urinary bladder model for radiation dose calculations. Task Group of the MIRD Committee, Society of Nuclear Medicine. *J Nucl Med.* 1999;40:102S-123S.

11. Forrer F, Krenning EP, Kooij PP, et al. Bone marrow dosimetry in peptide receptor radionuclide therapy with ^{177}Lu-DOTA(0),Tyr(3)-octreotate. *Eur J Nucl Med Mol Imaging.* 2009;36:1138-1146.

12. Kim MH, Kim HS, Rim KS, et al. The studies on the gastrin levels in the patients with renal failure. *Korean J Intern Med.* 1986;1:43-47.

13. Cimadamore A, Cheng M, Santoni M, et al. New prostate cancer targets for diagnosis, imaging, and therapy: Focus on prostate-specific membrane antigen. *Front Oncol.* 2018;8:653.

14. Afshar-Oromieh A, Avtzi E, Giesel FL, et al. The diagnostic value of PET/CT imaging with the ^{68}Ga-labelled PSMA ligand HBED-CC in the diagnosis of recurrent prostate cancer. *Eur J Nucl Med Mol Imaging.* 2015;42:197-209.

15. Dorff TB, Fanti S, Farolfi A, Reiter RE, Sadun TY, Sartor O. The evolving role of prostate-specific membrane antigen-based diagnostics and therapeutics in prostate cancer. *Am Soc Clin Oncol Educ Book.* 2019;39:321-330.

16. Roivainen A, Kahkonen E, Luoto P, et al. Plasma pharmacokinetics, whole-body distribution, metabolism, and radiation dosimetry of ^{68}Ga bombesin antagonist BAY 86-7548 in healthy men. *J Nucl Med.* 2013;54:867-872.

17. Nock BA, Kaloudi A, Lymperis E, et al. Theranostic perspectives in prostate cancer with the gastrin-releasing peptide receptor antagonist NeoBOMB1: Preclinical and first clinical results. *J Nucl Med.* 2017;58:75-80.

18. Gnesin S, Cicone F, Mitsakis P, et al. First in-human radiation dosimetry of the gastrin-releasing peptide (GRP) receptor antagonist ^{68}Ga-NODAGA-MJ9. *EJNMMI Res.* 2018;8:108.

19. Minamimoto R, Hancock S, Schneider B, et al. Pilot comparison of ^{68}Ga-RM2 PET and ^{68}Ga-PSMA-11 PET in patients with biochemically recurrent prostate cancer. *J Nucl Med.* 2016;57:557-562.

20. Sun B, Halmos G, Schally AV, Wang X, Martinez M. Presence of receptors for bombesin/gastrin-releasing peptide and mRNA for three receptor subtypes in human prostate cancers. *Prostate.* 2000;42:295-303.

21. Touijer KA, Michaud L, Alvarez HAV, et al. Prospective study of the radiolabeled GRPR antagonist BAY86-7548 for positron emission tomography/computed tomography imaging of newly diagnosed prostate cancer. *Eur Urol Oncol.* 2019;2:166-173.

22. Baum RP, Prasad V, Frischknecht M, Maecke HR, Reubi JC. Bombesin receptor imaging in various tumors: First results of Ga-68 AMBA PET/CT. *Eur J Nucl Med Mol Imaging.* 2007;34 Suppl 2:S119-436.

23. Thomas R, Chen J, Roudier MM, Vessella RL, Lantry LE, Nunn AD. In vitro binding evaluation of ^{177}Lu-AMBA, a novel ^{177}Lu-labeled GRP-R agonist for systemic radiotherapy in human tissues. *Clin Exp Metastasis.* 2008;26:105-119.

24. Artinyan A, Soriano PA, Prendergast C, Low T, Ellenhorn JD, Kim J. The anatomic location of pancreatic cancer is a prognostic factor for survival. *HPB (Oxford).* 2008;10:371-376.

25. Bakker IL, Konijnenberg M, Maina T, et al. From mouse to man: Translational properties of $^{67/68}$Ga-Sarabesin 3, a GRP-r antagonist, in mouse models versus primary prostate cancer patients. *J Nucl Med.* 2016;57:584-584.

26. Lymperis E, Kaloudi A, Sallegger W, et al. Radiometal-dependent biological profile of the radiolabeled gastrin-releasing peptide receptor antagonist SB3 in cancer theranostics: metabolic and biodistribution patterns defined by neprilysin. *Bioconjug Chem.* 2018;29:1774-1784.

FIGURES

FIGURE 1

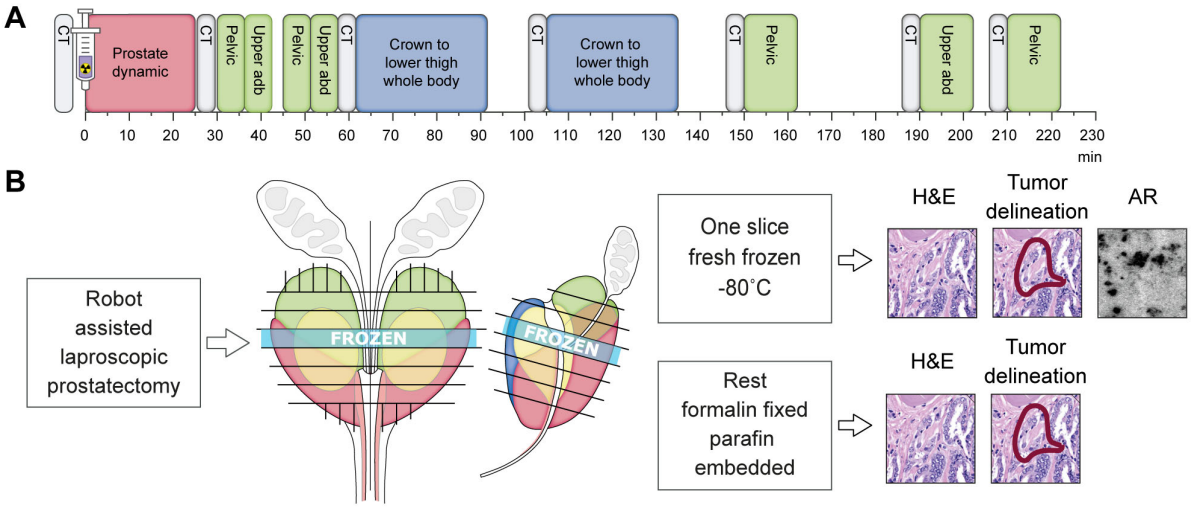

Schematic representation of research protocol. A: Protocol consisting of CTs (gray), dynamic scan (red), static images (green) and whole-body scans (blue). B: Tissue was cut in 4 mm sections, one was fresh frozen, remainder formalin fixed and paraffin embedded. Slides were stained with hematoxylin and eosin (H&E) and evaluated by the pathologist. Autoradiography (AR) was performed on slides of frozen sections.

FIGURE 2

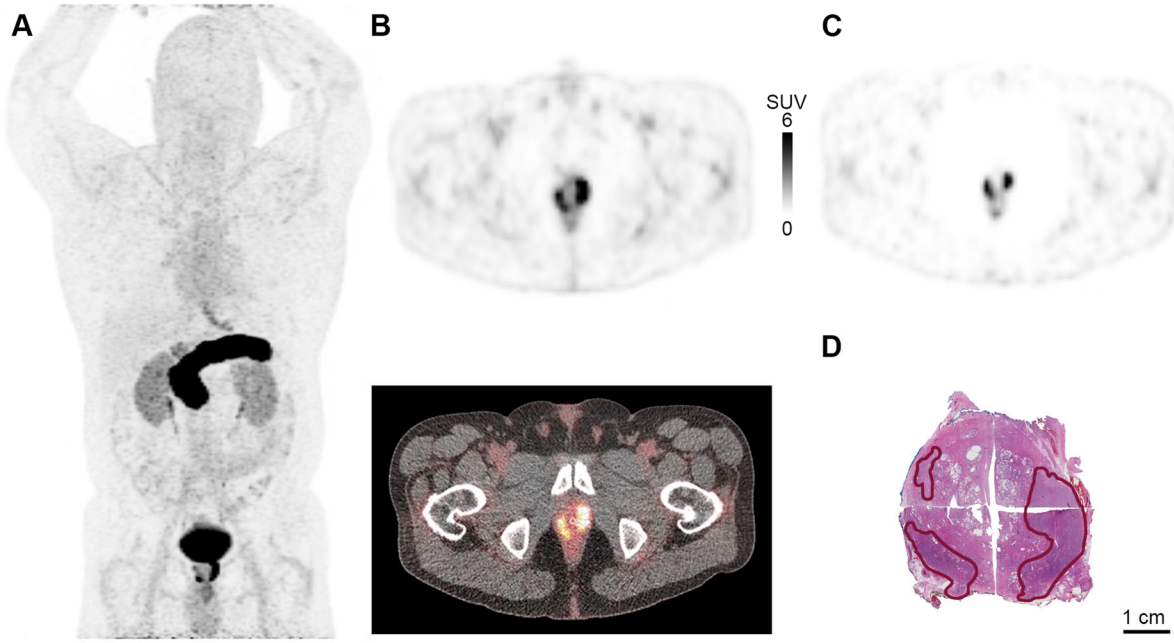

^{68}Ga-SB3 PET/CT-imaging of a primary prostate cancer patient. A large GS 3+4=7 tumor. A: Maximum intensity projection 60 min post injection (min.p.i.), B: On top PET imaging below PET/CT imaging, 60 min.p.i., tumor SUV_{MAX} 22.7. C: PET imaging 210 min.p.i. tumor SUV_{MAX} 20.0. E: corresponding histopathological slides with tumor delineation (red).

FIGURE 3

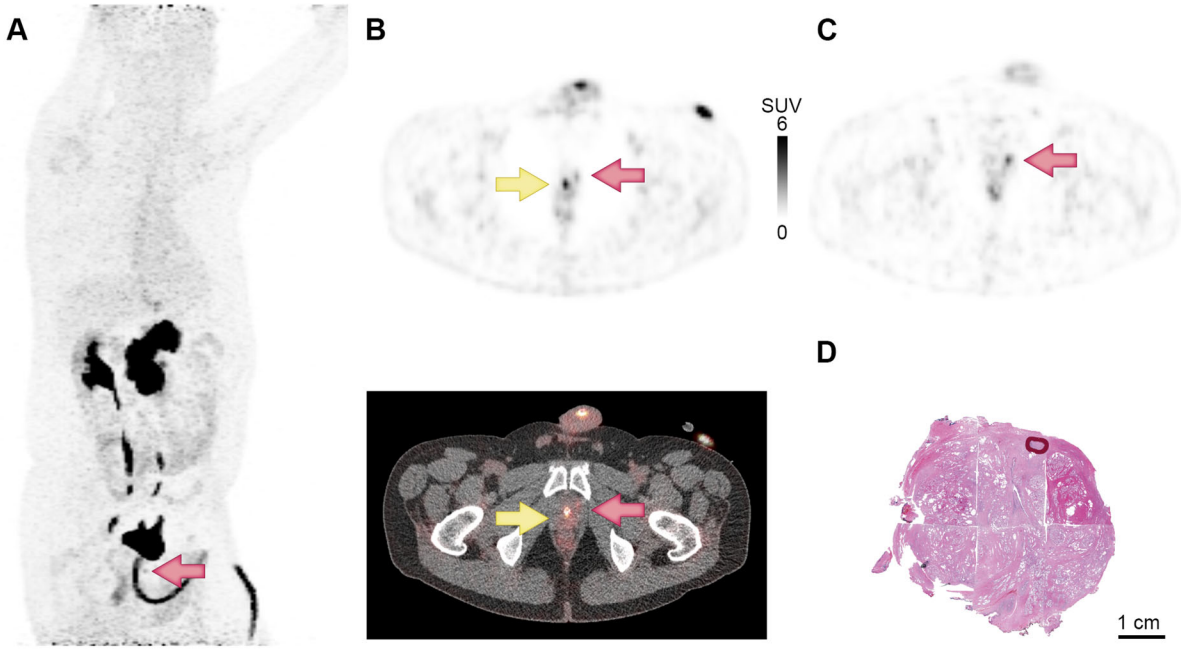

^{68}Ga-SB3 PET/CT-imaging of a primary prostate cancer patient. A very small GS 3+3=6 tumor (orange arrows), not detected in biopsies, however elevated PSA and family history of prostate cancer. Catheter (yellow arrow). A: Maximum intensity projection 60 min post injection (min.p.i.). B: On top PET imaging below PET/CT imaging, 60 min.p.i., tumor SUV_{MAX} 4.4. C: 210 min.p.i., catheter removed prior to scan, tumor SUV_{MAX} 4.3. D: corresponding histopathological slides with tumor delineation (red).

FIGURE 4

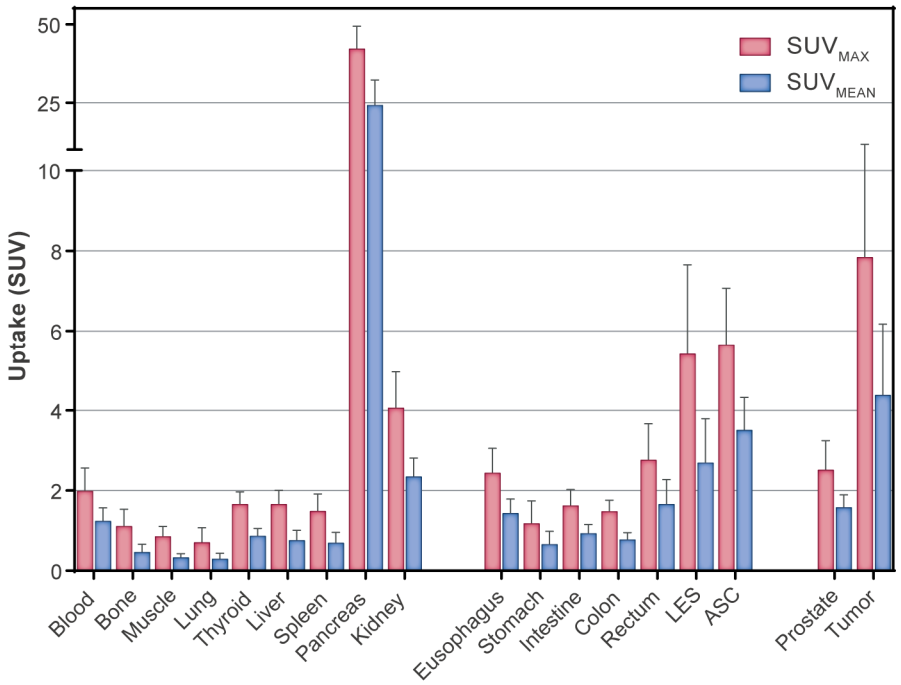

Biodistribution of ^{68}Ga-SB3 in therapy-naive prostate cancer patients. Biodistribution of physiological uptake and tumor uptake 60 min post injection. Mean SUV_{MAX} and SUV_{MEAN} are depicted with SD. LES: lower esophageal sphincter, ASC: anal sphincter complex.

FIGURE 5

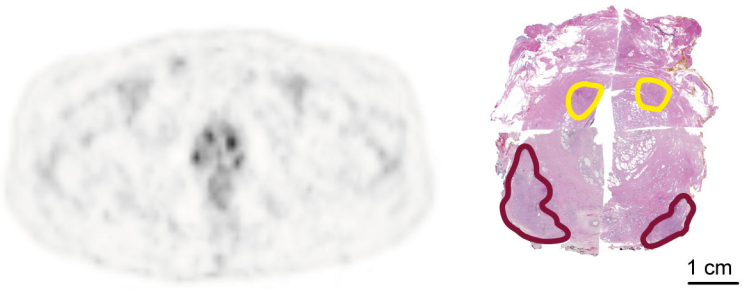

Imaging of prostate cancer and high-grade PIN in prostate cancer patient Left: 60 min post injection SUV6 PET image, showing almost equal uptake in PCa and PIN. Right: corresponding histopathology slide, tumor and PIN delineated, in red and yellow, respectively.

FIGURE 6

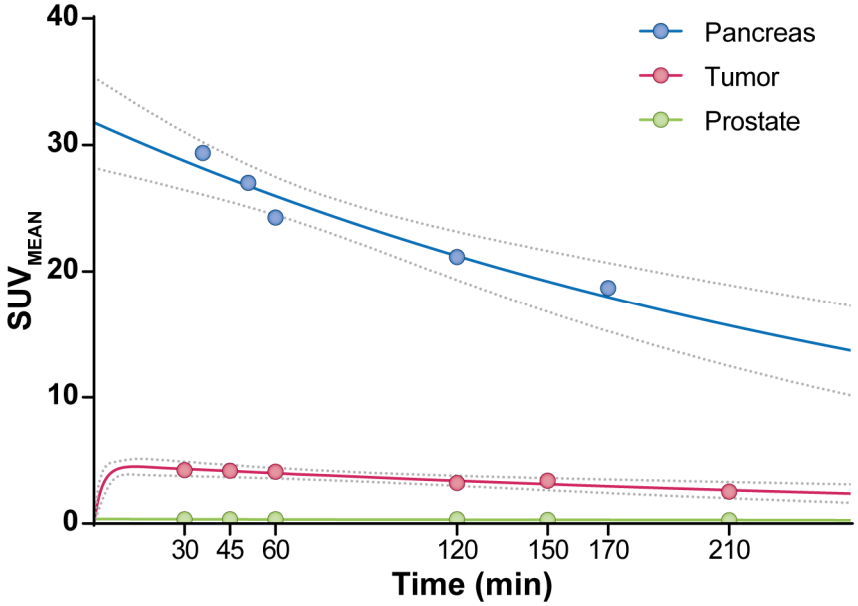

Pharmacokinetic pattern of ^{68}*Ga-SB3*. Excretion patterns from pancreas, tumor and normal prostate. Pancreas and prostate show excretion with a biological half time of 196 and 135 min, respectively. Excretion phase of tumor showed a half time of 235 min. Fits (solid lines) and 95% confidence intervals (dotted lines) are indicated.

TABLES

Table 1

Patient number	Side of prostate	Gleason Score	Autoradiography result	PET score	SUV_{MAX}	PET result	PIRADS	MRI result
1	L&R	3+4=7	++	5 5 4	22.7 14.4 5.9	TP	5	TP
2	L	3+4=7	+++	5	7.7	TP	4	TP
	R	3+3=6		5	17.0	TP	-	FN
3	L&R	4+3=7	+	5	13.3	TP	3	TP
	R	4+3=7		4	4.7	TP	-	FN
4	L&R	3+4=7	+	5 4	9.9 6.9	TP	3	TP
5	L	3+3=6	-	3	5.5	TP	5	TP
	R	4+4=8		5 5 3 4	5.5 6.3 3.2 5.3	TP	5	TP
6	L	3+4=7	-	4	5.8	TP	4	TP
	R	3+4=7		4	5.8	TP	3	TP
	L	PIN		5	4.9	FP		TN
	R	PIN		5	4.8	FP		TN
7	L	4+3=7	+	4	4.0	TP	5	TP
	R	4+3=7		5 5 4	5.5 5.5 3.7	TP	-	FN
8	L	3+3=6	+++	5	4.4	TP	n.a.	n.a.
	L	3+3=6		4	3.6	TP	n.a.	n.a.
9	L&R	3+4=7	-			FN	4	TP
10	L&R	3+3=6	-			FN	n.a.	n.a.

Tumor lesions per patient: PET, histopathology, autoradiography, MRI data. Correlation of tumor locations on pathology slides with focus spots found on PET. Also, MRI results and GRPr expression on autoradiography are mentioned. L: left, R: right, -: GRPr-negative, +: 0-33% GRPr-positive, ++: 33-66% GRPr-positive, +++: 66-100% GRPr-positive

TP: true positive, TN: true negative, FN: false negative, FP: false positive, n.a.: not available.

Graphical Abstract

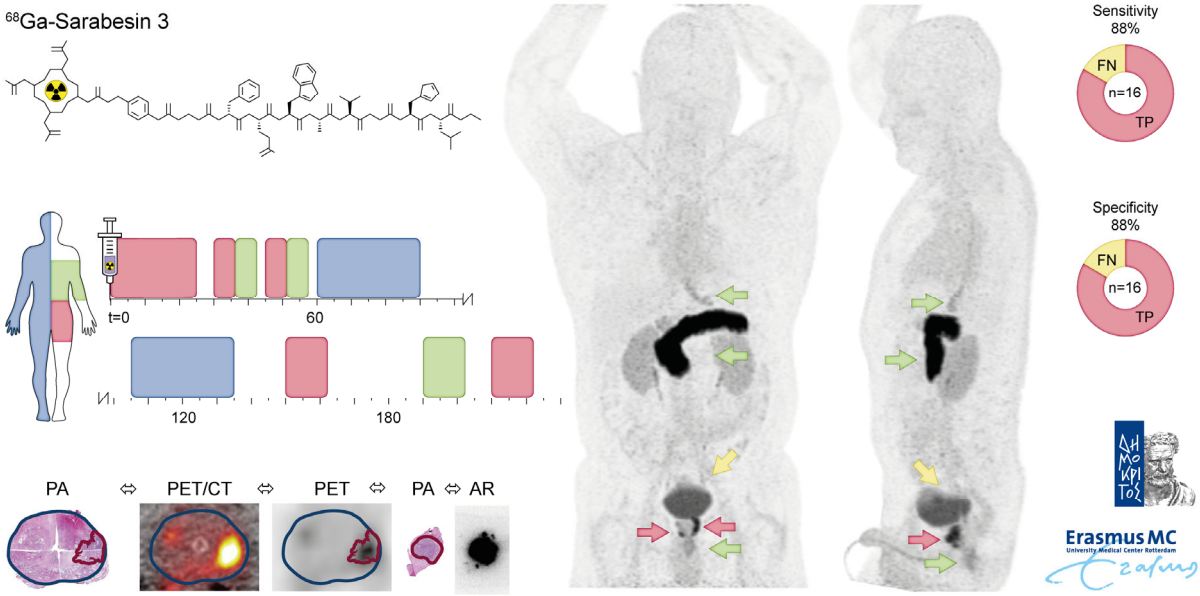

SUPPLEMENTAL FIGURES

Supplemental figure 1

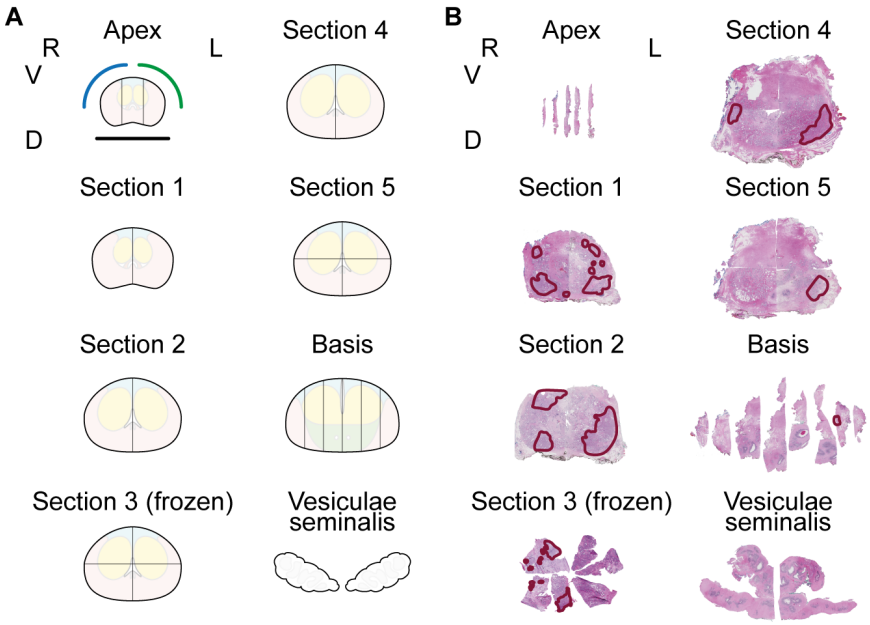

Tissue protocol. A: The basic edges of the resected prostate were marked with ink for anatomical reference and were freshly cut into 4 mm sections, following a pre-defined in-house protocol. The tissue that was not frozen was formalin-fixed (24-hrs) and paraffin-embedded. From every section 4 µm thick slides were obtained and stained with hematoxylin and eosin. Histopathology slides were scanned using a Hamamatsu NanoZoomer Digital Pathology (NDP) System (Hamamatsu Photonics K.K. Japan). B: Scanned images were reconstructed in transaxial whole-prostate images, scaled and stacked, based on previously described cutting protocols. L: left; R: right; V: ventral; D: dorsal.

Supplemental figure 2

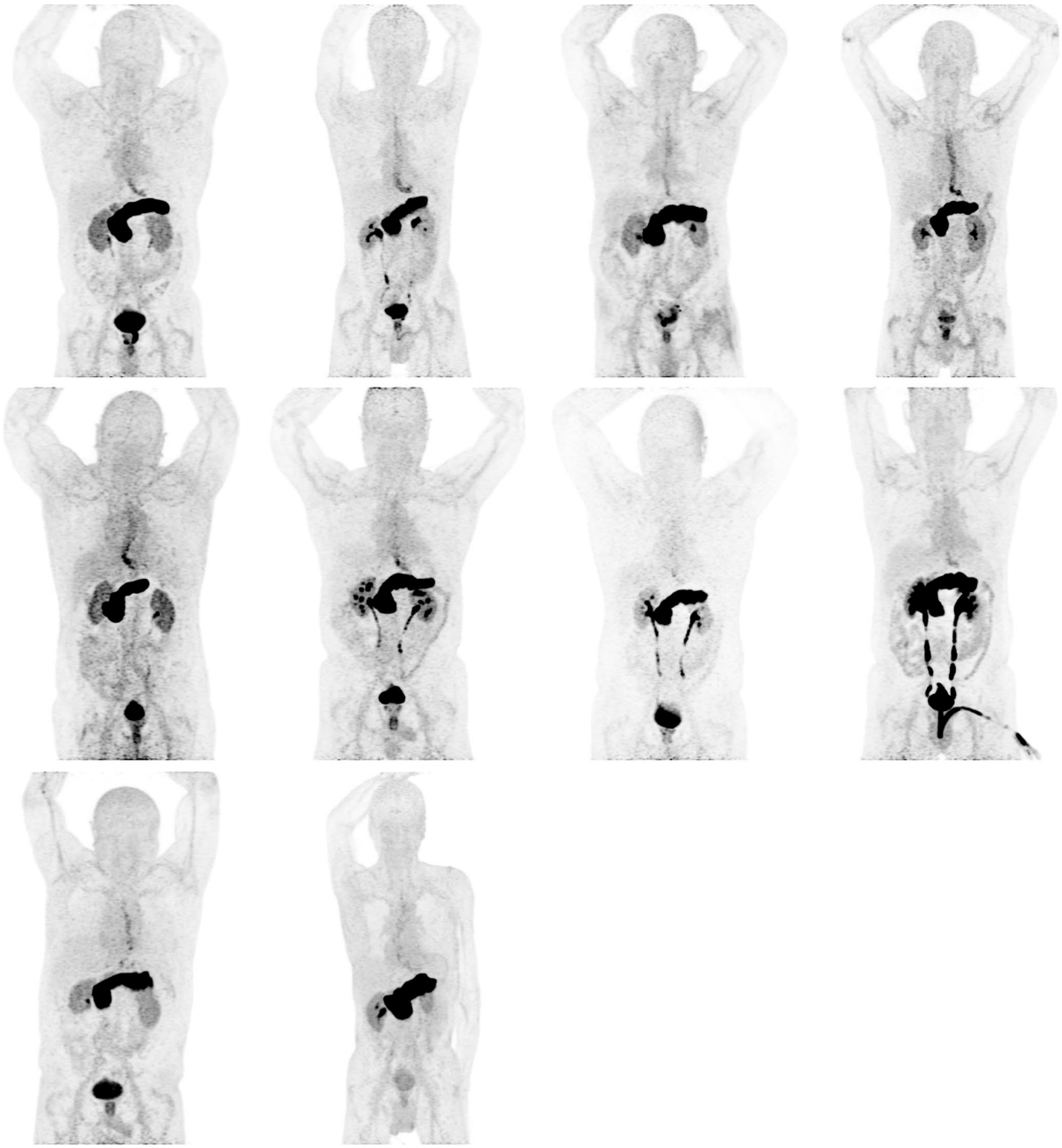

^{68}Ga-SB3 PET/CT-imaging maximum projection image of all patients. PET-positive patients on the first two rows, ranked from highest to lowest tumor uptake. PET-negative patients in bottom row. Scanned at 60 min post injection, scaled to SUV6. The 8th patient in this image did not receive an administration of furosemide, showing higher renal uptake.

Supplemental figure 3

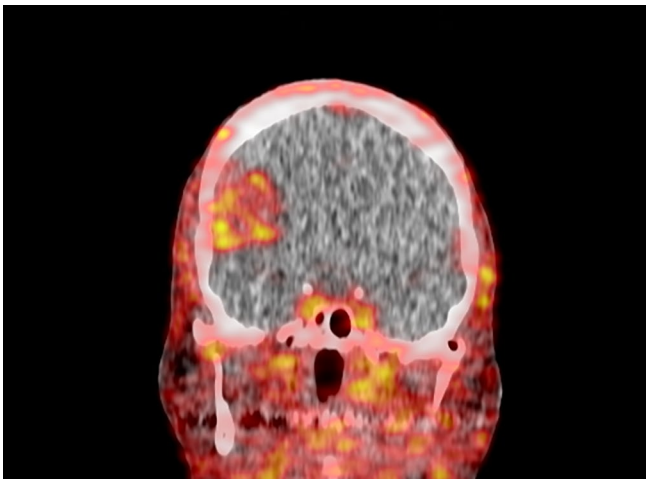

^{68}Ga-SB3 PET/CT-imaging of an MRI confirmed hemangioma. Image at 60 min post injection, scaled to 3 SUV. One unanticipated incidental finding was a sphere-like lesion within the cranium, SUV at level of blood, suspected of a hemangioma. Prior to the study the patient had opted to disclose all information deemed medically relevant by the nuclear physician. Therefore an MRI was performed which confirmed the diagnosis.

Supplemental figure 4

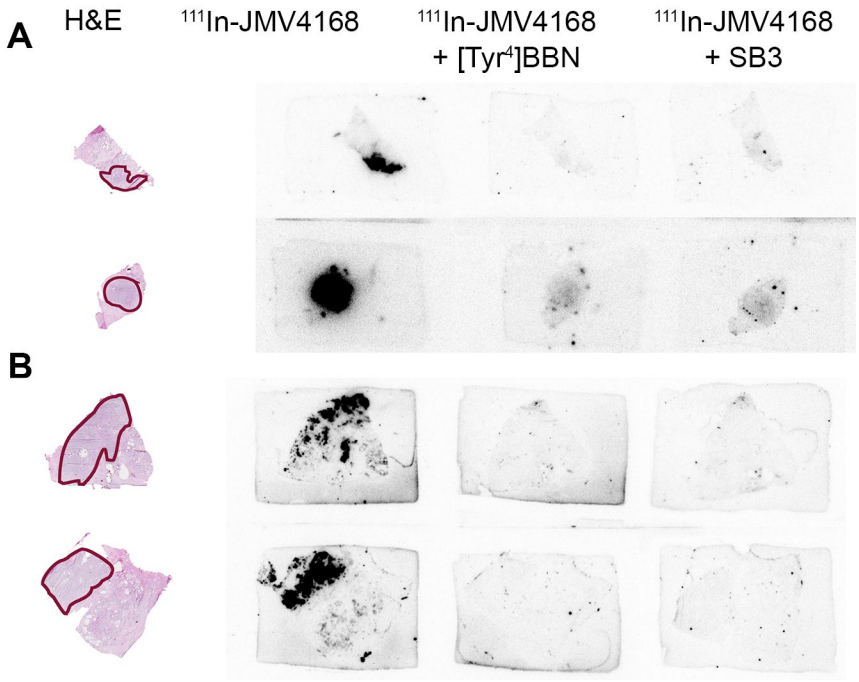

Autoradiography of fresh frozen samples with ^{111}In-JMV4168, confirming specific uptake in blocking studies. Fresh frozen sections of 10 µm were incubated for 1.0 h with 300 µL 10^{-9} M ^{111}In-JVM4168. To determine specific binding, subsequent slides were incubated with 300 µL 10^{-9} M ^{111}In-JVM4168 plus an excess of unlabeled peptide, either 10^{-6} M Tyr^4-BBN as the gold standard or 10^{-6} M SB3. A: example of a 100% GRPr-expressing tumor. B: example of a 50% GRPr-expressing tumor.

Supplemental figure 5

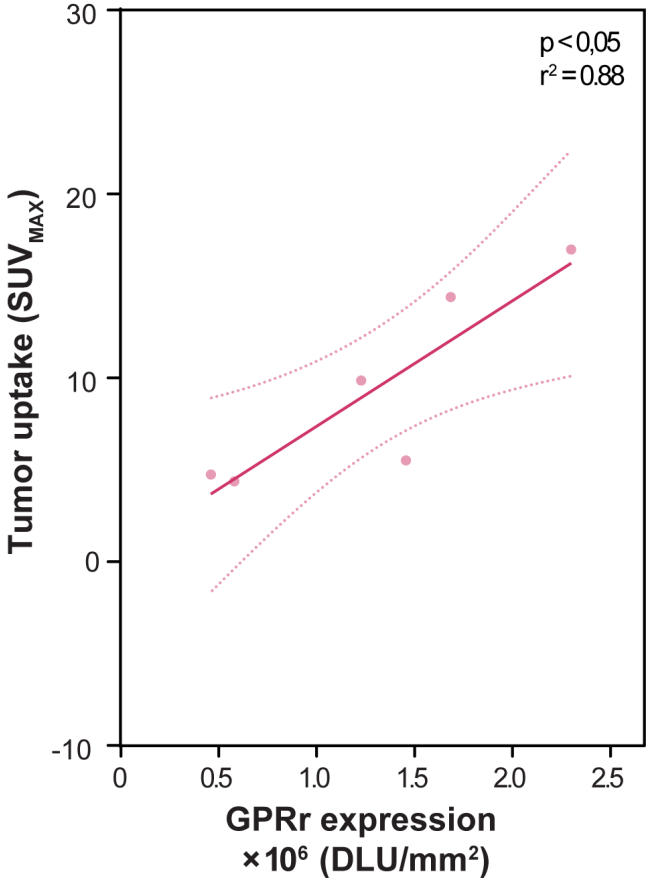

Correlation between GRPr expression on autoradiography and tumor uptake on PET. GRPr expression of tumor areas on autoradiography is expressed as DLU/mm^2 and tumor uptake on PET as SUV_{MAX} at 60 min post injection.

SUPPLEMENTAL TABLES

Supplemental table 1

Timepoint	Scan area	Number of bed positions	Minutes per bed position	Number of scans performed	Exact scan time ± SD (min)
0	Pelvic	1	List mode	10	1 ± 1
30	Pelvic	1	6	10	31 ± 4
36	Upper abdomen	1	6	10	39 ± 4
45	Pelvic	1	6	10	47 ± 4
51	Upper abdomen	1	6	9	53 ± 1
60	Whole body	7	4 pelvic area 6	10	64 ± 2
120	Whole body	7	4 pelvic area 6	10	121 ± 4
150	Pelvic	1	12	10	158 ± 8
170	Upper abdomen	1	12	5	169 ± 4
210	Pelvic	1	12	10	211 ± 9

Scan protocol. The tracer was administered using a Rad-Inject automated system in 5 ± 2 min. Just prior to the start of injection a 20 min dynamic PET list mode acquisition was started.

All PET acquisitions were preceded by a low dose CT scan, using 120 kVp and 40 ref mAs for the static PET scans or 120kVp and 20 ref mAs for the whole-body PET scans. PET images were reconstructed using an ordered subset expectation maximization algorithm using resolution recovery, time-of-flight information, 3 iterations, 21 subsets and a 3 mm post-reconstruction Gaussian filter. Attenuation and scatter correction were applied during reconstruction.

In 1 patient a 51 min pelvic scan was omitted because of catheter discomfort. Scans were performed within a timeframe of 5 min of planned time, except for the last scan, which was performed within 10 min of the planned time.

Supplemental table 2

Timepoint	Blood for pharmacokinetics	Blood for stability	Urine for pharmacokinetics	Urine for stability
0	Yes		Yes	
5	Yes	Yes		
10	Yes	Yes		
20	Yes			
30	Yes		Yes	Yes
45	Yes			
60	Yes		Yes	Yes
100	Yes			
140	Yes			
180	Yes		Yes	

Protocol for blood and urine samples. Ten 3 mL venous blood samples were collected during scanning. All urine was collected, although highly diluted by continuous flush, in time intervals 0-30 min, 30-60, 60-90 and 90-180 min, the volumes were registered, and 3 mL samples were drawn. Radioactivity in blood and urine and standards was measured in a gamma-counter. In vivo degradation of the radiotracer was assessed by HPLC.

Supplemental table 3

Patient number	iPSA (µg/l)	cT	TRUS volume (cc)	Number of positive biopsy cores	Gleason Score of biopsy cores	Change of lymph node involvement
1	13,4	T3a	32	8 of 9	3+4=7	0.23
2	5,9	T1c	24	4 of 12	3+4=7	0.03
3	24,8	T2a	80	3 of 16	4+3=7	0.12
4	24,8	T2a	27	4 of 13	3+4=7	0.08
5	17	T1c	31	5 of 8	3+4=7	0.08
6	12,9	T1c	38	3 of 9	3+3=6	0.02
7	6,4	T2c	14	3 of 6	4+4=8	0.36
8	23	T1c	74	1 of 36	3+3=6	0.01
9	10,3	T2a	62	6 of 16	3+4=7	0.05
10	4	T2a	49	3 of 9	3+4=7	0.05
excluded	19,6	T3a	120cc	1 of 8	3+3=6	0.08

Patient Characteristics. Inclusion criteria were male patients of 18 years and older; histologically confirmed prostate cancer, no clinical suspicion of metastasis; scheduled for radical prostatectomy; capable of cooperating with imaging procedure and follow-up; World Health Organization performance status 0-2; a signed and dated informed consent. Exclusion criteria were: current severe and/or uncontrolled and/or unstable other medical disease (e.g. poorly controlled diabetes, unstable and uncontrolled hypertension, chronic renal or hepatic disease, severe pulmonary disease); other malignancies (except local skin cancer); chemotherapy, radiotherapy, or anti-hormonal therapy prior to study; significant cardiac arrhythmia current or in patient history; prior NYHA class III-IV cardiac disease or concurrent congestive heart failure; prior major thoracic and/or abdominal surgery from which the patient has not yet recovered; known sensitivity to the study drug or components of the preparation; other concurrent investigational drugs within the past four weeks or planned in the period until four weeks after administration of gallium-68 labeled SB3 (^{68}Ga-SB3, ^{68}Ga-DOTA-*p*-aminomethylaniline-diglycolic acid-DPhe-Gln-Trp-Ala-Val-Gly-His-Leu-NHEt); other condition that, in the opinion of the investigators, would make the patient unsuitable for this clinical trial. Patients were not selected on Gleason Score in biopsy specimens.

Use of 5-alfa-reducatase inhibitors had to be discontinued two weeks before the study. These inhibitors reduce the conversion of testosterone to dihydrotestosterone, which is a stimulus for

prostatic hyperplasia. Effects of these inhibitors on gastrin releasing peptide receptor (GRPr) expression status are not yet known.

If lower limit of detection was reached, defined by inability to evaluate visualization of physiological uptake, the patient was excluded from the study and replaced.

When chance of lymph node involvement was > 0,05 extended pelvic lymph node dissection was performed.

Supplemental table 4

	0 min	30-36 min	45-51 min	60 min	120 min	150 min	170 min	210 min
Blood	3.7 ± 0.7	2.5 ± 0.8	2.1 ± 0.8	2.0 ± 0.6	1.6 ± 0.4	1.4 ± 0.6	1.8 ± 1.1	1.4 ± 0.8
Bone	1.1 ± 0.5	1.3 ± 0.7	1.3 ± 0.6	1.1 ± 0.4	1.4 ± 0.7	1.2 ± 0.8	1.1 ± 0.8	1.5 ± 1.8
Muscle	0.9 ± 0.2	1.1 ± 0.4	1.1 ± 0.4	0.8 ± 0.3	0.8 ± 0.3	0.6 ± 0.3	0.7 ± 0.4	0.8 ± 0.5
Lung				0.7 ± 0.4	0.6 ± 0.3			
Heart				2.0 ± 0.5	1.8 ± 0.8			
Thyroid				1.6 ± 0.3	1.2 ± 0.4			
Liver		2.1 ± 0.3	1.7 ± 0.5	1.6 ± 0.4	1.6 ± 0.5		1.4 ± 0.3	
Spleen		1.9 ± 0.3	1.7 ± 0.5	1.5 ± 0.4	1.6 ± 0.8		1.3 ± 0.3	
Pancreas		49.2 ± 14.8	44.9 ± 15.7	42.1 ± 15.7	36.3 ± 13.3		31.3 ± 14.8	
Kidney		6.3 ± 2.3	4.7 ± 1.6	4.1 ± 0.9	3.9 ± 1.2		3.7 ± 0.8	
Esophagus				2.4 ± 0.6	2.6 ± 0.6			
Stomach		1.2 ± 0.4	1.0 ± 0.5	1.2 ± 0.6	1.3 ± 0.7		1.4 ± 0.5	
Intestine		2.2 ± 0.7	2.0 ± 0.6	1.6 ± 0.4	1.8 ± 0.8		1.6 ± 0.6	
Colon		1.7 ± 0.4	1.5 ± 0.5	1.5 ± 0.3	1.6 ± 0.6		1.3 ± 0.6	
Rectum	1.6 ± 0.7	2.3 ± 0.9	2.6 ± 1.0	2.8 ± 0.9	2.7 ± 0.9	2.3 ± 0.7		2.4 ± 1.3
Lower esophageal junction		5.1 ± 1.6	5.2 ± 1.9	5.4 ± 2.2	5.2 ± 2.3		6.3 ± 1.7	
Anal sphincters	2.8 ± 0.8	5.1 ± 1.5	5.7 ± 1.5	5.6 ± 1.4	5.8 ± 1.5	5.9 ± 2.1		5.1 ± 1.8
Prostate	2.7 ± 0.5	2.3 ± 0.6	2.4 ± 0.9	2.5 ± 0.7	1.9 ± 0.6	1.7 ± 0.6		1.3 ± 0.5
Tumor	5.4 ± 2.7 (2.9-15.8)	7.2 ± 5.2 (2.5-25.9)	7.0 ± 4.6 (4.0-20.8)	7.1 ± 4.8 (3.0-22.7)	6.6 ± 5.4 (1.8-21.4)	6.5 ± 4.3 (2.3-19.1)		5.8 ± 4.7 (1.7-20.0)

Biodistribution of ^{68}Ga-SB3 in therapy-naive prostate cancer patients. Biodistribution of physiological uptake and uptake in all PET positive tumor lesions, based on VOIs on PET/CT images. SUV_{MAX}± SD (for tumor range) is reported.

Volumes-of-interest (VOI) were drawn on ^{68}Ga-SB3 PET/CT fusion images using OsiriX. Volumes of VOIS were in muscle (m. gluteus maximus, m. latissimus dorsi), liver, spleen and lung 10 cm^3; in bone (vertebra Th10, sacrum S2-S3), cortex of both kidneys, pancreas head, pancreas corpus 5 cm^3; in anal sphincter complex, renal pelvis (urine), pancreas tail, aorta (blood) 3 cm^3; and in thyroid, esophagus (upper sphincter, wall, lower sphincter), stomach wall, intestine wall, colon wall, rectum wall 1 cm^3. In suspected tumor lesions and normal prostate VOIs of 0.5 cm^3 were drawn.

Supplemental table 5

Organs	Residence times h mean ± SE	Absorbed dose mGy/MBq
Adrenals	6.21E-04*	1.08E-02
Brain	1.46E-03	4.80E-04
Colon wall	2.15E-05±9.95E-06	4.58E-03
Esophagus	2.35E-06±1.41E-06	2.75E-03
Eyes	6.23E-07*	3.27E-04
Gallbladder wall	7.97E-04*	1.65E-02
Heart wall	6.55E-03±3.65E-03	8.24E-03
Kidneys	4.82E-02±3.10E-02	5.28E-02
Left colon wall	2.15E-05±9.95E-06	2.76E-03
Liver	4.39E-02±2.15E-02	1.25E-02
Lung	5.89E-03±4.18E-03	3.57E-03
Pancreas	7.94E-02±3.35E-02	1.98E-01
Prostate	4.45E-04±6.00E-05	2.95E-02
Recto-sigmoid colon wall	1.75E-05±1.57E-05	9.74E-03
Red (active) bone marrow	9.45E-02±2.40E-02	1.57E-02
Right colon wall	2.15E-05±9.95E-06	3.81E-03
Small intestine wall	6.60E-05±2.62E-05	6.59E-03
Spleen	4.37E-03±2.12E-03	1.07E-02
Stomach wall	7.00E-06±1.10E-05	5.29E-03
Testes	1.57E-04*	1.60E-03
Thymus	1.24E-04*	1.78E-03
Thyroid	3.42E-04±1.36E-04	6.44E-03
Renal pelvis	7.75E-03±1.46E-02	1.34E-01
Urinary bladder wall	2.47E-01±1.53E-01	1.16E-01

Residence times and absorbed doses in organs of interest of ^{68}Ga-SB3 in male adults. Residence times calculated from time activity curves and organ-absorbed doses calculated in IDAC2.1, assumed 1 h voiding. *from standard values of ICRP tables.